第 30 卷第 6 期
2014 年 6 月

无 机 化 学 学 报
CHINESE JOURNAL OF INORGANIC CHEMISTRY

Vol.30 No.6
1403-1412

氧化体系对 $LiFePO_4$ 化学脱锂的影响

孙孝飞 徐友龙* 陈国岗 李 彤 贾莫瑞 李 璐

(西安交通大学电子陶瓷与器件教育部重点实验室,国际电介质研究中心,西安 710049)

摘要: 化学脱锂被广泛用于研究锂离子电池活性材料脱锂前后结构与性能的相互关系。本文通过改进的固相烧结法制备了粒径约 12.61 μm 的超大颗粒 $LiFePO_4$ 粉末,分别在乙腈和水溶液体系中采用 NO_2BF_4 和 $K_2S_2O_8$ 作为氧化剂对其进行化学脱锂,探讨了两种氧化体系所得到的 $FePO_4$ 在晶体结构、颗粒形貌和电化学性能等方面的差异。实验结果表明,溶剂亦高度参与了脱锂反应,特别是 $K_2S_2O_8$ 氧化得到的 $FePO_4$ 中存在大量 O-H 基团,除未被烘干的 H_2O 外,说明 $Li_xFePO_4(0\leqslant x\leqslant 1)$在强氧化性水溶液中可能存在质子嵌入。伴随反应过程中搅拌分散、物质溶解、化学脱锂和质子嵌入等协同作用,使所得 $FePO_4$ 的晶胞体积和颗粒尺寸明显减小,最终导致充放电曲线畸变、阻抗增大和容量降低。虽然低温退火可去除大部分 O-H,但是不可逆的结构和形貌改变导致电池性能依然无法与初始 $LiFePO_4$ 相比。与此相反,采用 NO_2BF_4 有机溶液体系脱锂得到的 $FePO_4$ 没有发生明显的结构、形貌和性能变化,因而是一种更加可靠的 $LiFePO_4$ 化学脱锂体系。

关键词: 磷酸铁锂; 化学脱锂; 质子嵌入; 正极材料; 锂离子电池; 能量存储

中图分类号: O646 **文献标识码**: A **文章编号**: 1001-4861(2014)06-1403-10

DOI: 10.11862/CJIC.2014.160

Influence of Oxidation System on Chemical Delithiation of $LiFePO_4$

SUN Xiao-Fei XU You-Long* CHEN Guo-Gang LI Tong JIA Ming-Rui LI Lu

(*Electronic Materials Research Laboratory, Key Laboratory of the Ministry of Education & International Center for Dielectric Research, Xi'an Jiaotong University, Xi'an* 710049, *China*)

Abstract: Chemical delithiation is widely used in literature to study the structure-property-performance relationship of olivine $LiFePO_4$ before/after lithium extraction, but the influence of oxidation system on the structure, morphology and electrochemical performance of the resulted Li_xFePO_4 $(0\leqslant x<1)$ is seldom noticed. In this paper, large particle $LiFePO_4$ is synthesized via a modified solid-state reaction method and is chemically delithiated by NO_2BF_4 in acetonitrile or by $K_2S_2O_8$ in an aqueous solution. Solvents are found highly involved in chemical delithiation of $LiFePO_4$, and significant O-H groups are identified in $FePO_4$ derived by $K_2S_2O_8$. Moreover, proton insertion into the crystal lattice of Li_xFePO_4 $(0\leqslant x\leqslant 1)$ is demonstrated possible in such highly oxidative aqueous solutions. The synergism of dispersion, dissolution, delithiation, and more importantly protonation induces serious structure and morphology change to so-obtained $FePO_4$ and makes the particle size much smaller. Consequently, the specific discharge capacity is dramatically decreased with increased charge transfer impedance, and the charge/discharge curves are transformed to slope-like profiles. Although these protons (including residual water and hydroxyls) could be removed by low temperature annealing, the battery performance can't be fully recovered due to the irreversible structure and morphology change. On the contrary, there is no obvious proton incorporation during chemical delithiation of $LiFePO_4$ by NO_2BF_4 in organic solutions, which leads to $FePO_4$ with almost invariant structure, morphology and performance comparing to pristine $LiFePO_4$.

Key words: lithium iron phosphate; chemical delithiation; proton insertion; cathode material; lithium ion battery; energy storage

收稿日期:2013-09-17。收修改稿日期:2013-12-19。

国家自然科学基金(20804030、50902109)、高等学校博士点专项科研基金(20110201130005)资助项目。

*通讯联系人。E-mail:ylxu@mail.xjtu.edu.cn;会员登记号:E190005546f。

0 Introduction

Since the pioneering work by Padhi et al.[1] in 1997, olivine $LiFePO_4$[2-3] has been intensively studied as a promising cathode material[4-5] for lithium ion batteries (LIBs) due to its unique advantages such as high specific capacity (theoretically 170 $mAh \cdot g^{-1}$), high energy density, low cost and environmental benignity. Moreover, the olivine structure is stable during charge/discharge because of the inductive effect of PO_4^{3-} polyanions[6], which endows $LiFePO_4$ the high safety merit and long-life cycling trait when used in high efficiency energy storage applications[7] such as electric vehicles (EVs), hybrid electric vehicles (HEVs) and plug-in hybrid electric vehicles (PHEVs)[8]. However, the low intrinsic conductivity hinders its further industrial commercialization. Particle downsizing[9-11], surface coating[12-14] and bulk doping[15-17] are then employed to overcome this shortcoming. And a high power $LiFePO_4$ with excellent rate performance has already been reported[18].

On the other hand, it is of great importance to understand the structure-property-performance relationship before and after charge/discharge, so as to design novel materials for high performance LIBs accordingly. Lithium ions (Li^+) were predicted[19-20] to diffuse in one dimensional tunnels along [010] direction[21], which was later verified experimentally by Yamadas group[22]. Meanwhile, shrink-core[23], platelet type[24-25], domino cascade[26] models were introduced successively to interpret the two-phase reaction process during charge/discharge. Moreover, solid solution phase[27-28] was found at the beginning of charge/discharge. Gu[29] et al. also observed the lithium staging phenomenon in partially delithiated $LiFePO_4$ analogously in layered intercalation compounds by aberration-corrected scanning transmission electron microscopy (STEM). Recently, *ab-initio* computation[30-31] revealed the suppression of phase separation due to the non-equilibrium Li incorporation during discharging.

Therefore, it is vital to get reliable intermediate Li_xFePO_4 ($0<x<1$) as well as the end $FePO_4$ for above research. Electrochemical lithium extraction is ideal but constrained by the low yield and complex process with contamination from binder and conductive additives. As a simple approximation, chemical delithiation[28] has been successfully applied to get large quantity Li_xFePO_4 ($0 \leqslant x < 1$) with desired compositions. On basis of that, the lithium diffusion path and the two-phase reaction during charge/discharge as well as the solid solution behavior were able be verified. Besides, Lin et al.[32] showed inhomogeneous phase progression in single crystal $LiCoO_2$ by chemical delithiation, and Wu[33] et al. found the vanishing of super lattice in $(1-z)Li[Li_{1/3}Mn_{2/3}]O_2$-$zLi[Mn_{0.5-y}Ni_{0.5-y}Co_{2y}]O_2$ on extracting a significant amount of lithium during chemical delithiation due to the loss of ordering between the Li^+ and the transition metal ions. Among the family of this powerful technique, nitronium tetrafluoroborate (NO_2BF_4)[34] in acetonitrile and potassium persulfate ($K_2S_2O_8$)[35] in an aqueous solution are the two common oxidation systems in literature because of the appropriate redox potential in addition with easy operation. To our knowledge, the difference between $FePO_4$ delithiated by the two oxidation systems is seldom identified. In this paper, we report the structure, morphology and performance difference of $FePO_4$ delithiated from large particle $LiFePO_4$ by NO_2BF_4 in acetonitrile and $K_2S_2O_8$ in water respectively for the first time. Moreover, proton insertion into the crystal lattice of Li_xFePO_4 ($0 \leqslant x \leqslant 1$) is found possible in highly oxidative aqueous solutions although previous calculation indicates that olivine $LiFePO_4$ is unfavorable of protonation[36].

1 Experimental Section

1.1 Materials Preparation

Pristine $LiFePO_4$ was prepared by a modified solid-state reaction route. The precursors of lithium carbonate Li_2CO_3, iron oxalate $FeC_2O_4 \cdot 2H_2O$ and ammonium dihydrogen phosphate $NH_4H_2PO_4$ were mixed together stoichiometrically and were ball-milled for 12 h in acetone. After drying at 80 ℃ for 4 h, they were grounded in a mortar for 1 h. The mixture was then thermally decomposed at 350 ℃ for 6 h under an

argon (Ar) flow. The obtained powder was regrounded and mixed manually again for 2 h. In order to get large particle $LiFePO_4$, it was pressed into pellets followed by heating at 800 ℃ for 24 h under Ar protection.

The pristine $LiFePO_4$ was chemically delithiated either by NO_2BF_4 or by $K_2S_2O_8$ When the former was used as the oxidant, 1.7 g NO_2BF_4 (100% excess) was dissolved in 100 mL acetonitrile and 1 g $LiFePO_4$ was added in dropwise. The mixture was vigorously stirred for 30 h at ambient temperature. The products were filtered by methanol (CH_3OH) for several times and were dried at 80 ℃ for 12 h under vacuum. The so-obtained sample is denoted as $FePO_4$-N hereafter. Similar process was used to delithiate $LiFePO_4$ by $K_2S_2O_8$. 1.7 g $K_2S_2O_8$ (100% excess) and 1 g $LiFePO_4$ were dissolved in 100 mL deionized water. The mixture was stirred for 30 h allowing the equilibrium to be reached. It was then filtered alternatively by water and ethanol for several times with the latter at the end, and was dried in a vacuum oven at 80 ℃ for 12 h. The collected sample is designated as $FePO_4$-K hereafter. In order to remove the inserted protons including residual water and hydroxyls, $FePO_4$-K was post annealed at 300 ℃ for 24 h in Ar atmosphere and was cooled naturally to room temperature. It is assigned as $FePO_4$-K-AN in the rest of the paper.

1.2 Materials Characterization

Powder X-ray diffraction (XRD) was conducted on an Xpert Pro (PANalytical) with Cu $K\alpha$ radiation. Rietveld refinement on the XRD data was performed by the High Score Plus software. The particle morphology was observed by scanning electron microscopy (SEM, VEGA3 LMH) and transmission electron microscopy (TEM, JEM 2100). The particle size distribution was obtained by laser particle size analyzer in Xi′an Maxsun Kores New Materials Co., LTD. The Li/Fe/P ratio was characterized by inductively coupled plasma atomic emission spectroscopy (ICP-AES) also with the help of Xi′an Maxsun Kores New Materials Co., LTD, and was double checked by energy dispersive X-ray detection (EDX, INCA ENERGY250) attaching to the aforementioned SEM. Fourier transform infrared spectroscopy (FTIR, Bruker, VERTEX 70) was carried out with pellets made of KBr and the samples. The thermal behavior of $FePO_4$-K was investigated by thermogravimetry-differential scanning calorimetry (TG-DSC, STA 449C) at a heating rate of 5 ℃·min^{-1} from room temperature to 400 ℃ under N_2 protection while the cooling process was recorded at 10 ℃·min^{-1}.

1.3 Battery Performance

A homogeneous slurry of the active material ($LiFePO_4$ or $FePO_4$, 70wt%), conducting carbon (acetylene black, 20wt%) and binder (PVDF, 10wt%) in *N*-Methyl-2-Pyrrolidone (NMP) was casted onto a pretreated aluminum foil by the doctor blade technique. The cathode was then dried under vacuum at 80 ℃ for 12 h. CR2016 coin cells were fabricated in an Ar-filled glove box. Lithium metal was used as the anode, and the electrolyte was 1 mol·L^{-1} $LiPF_6$ in EC/DMC (1∶1, *V*/*V*). The batteries were charge/discharged on a CT2001A Land Battery Testing System to evaluate their performance. The electrochemical impedance spectroscopy (EIS) was carried out on a Versatile Multichannel Galvanostat 2/Z (VMP2, Princeton Applied Research). An ac voltage signal of ±5 mV was used in the frequency range from 10^{-2} to 10^5 Hz.

2 Results and Discussion

Lithium could be removed from $LiFePO_4$ by chemical delithiation with NO_2BF_4 and $K_2S_2O_8$ according to equation (**1**) and (**2**), respectively.

$$LiFePO_4+NO_2BF_4 \rightarrow FePO_4+LiBF_4+NO_2 \quad (\mathbf{1})$$

$$2LiFePO_4+K_2S_2O_8 \rightarrow 2FePO_4+Li_2SO_4+K_2SO_4 \quad (\mathbf{2})$$

Fig.1 shows the XRD patterns of pristine $LiFePO_4$, chemically derived $FePO_4$ by NO_2BF_4 ($FePO_4$-N) and that by $K_2S_2O_8$ ($FePO_4$-K). Each sample agrees well with its reference pattern without detectable impurities. Belonging to the space group of *Pnma*, the as-prepared $LiFePO_4$ occupies a slightly distorted hexagonal close packing with LiO_6 octahedra, FeO_6 octahedra, and PO_4 tetrahedra. After delithiation, it can be seen by ICP-AES (Table 1) that almost all lithium are removed taking into account of the

Table 1 Li/Fe/P ratios of $LiFePO_4$, $FePO_4$-N and $FePO_4$-K characterized by ICP-AES and EDX, respectively

Samples	Li/Fe/P ratio(ICP-AES)	Fe/P ratio(EDX)
Pristine $LiFePO_4$	1.04:0.97:1	0.97:1
$FePO_4$-N	0.01:0.96:1	0.96:1
$FePO_4$-K	0.01:0.95:1	0.94:1

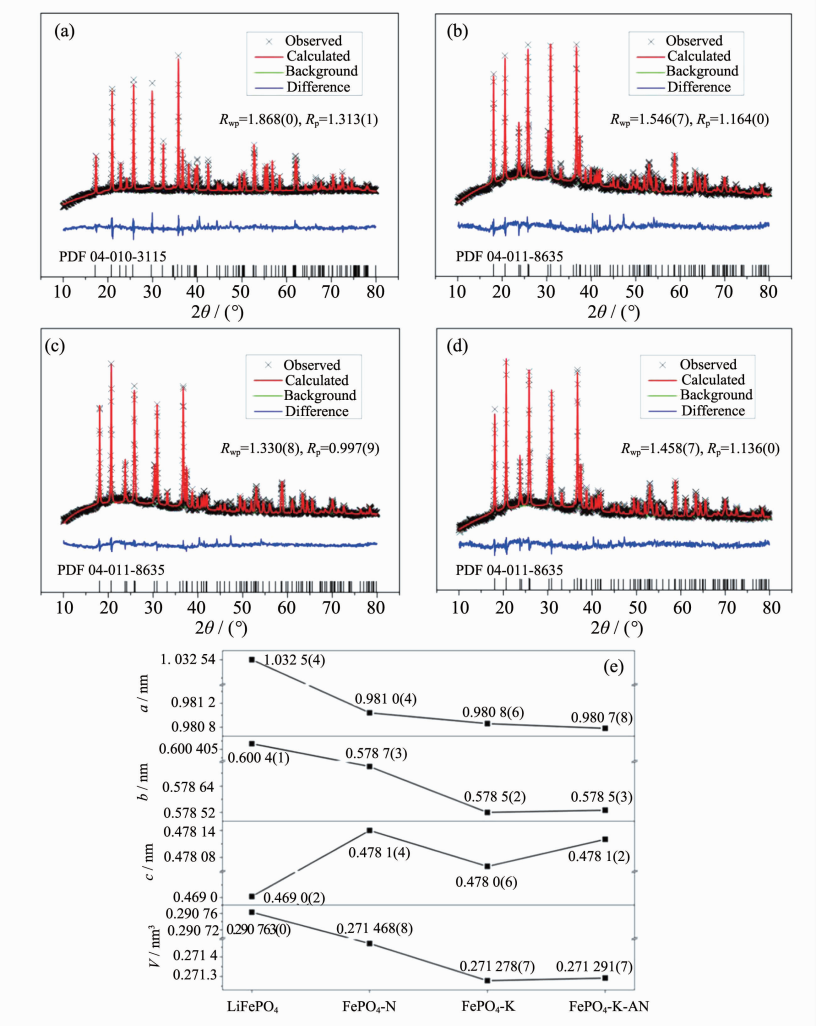

Fig.1 Rietveld refinement on XRD patterns of pristine $LiFePO_4$ (a), $FePO_4$-N (b), $FePO_4$-K (c) and $FePO_4$-K-AN (d). The calculated lattice parameters are summarized in (e). The vertical lines in the bottom of (a)-(d) indicate the reference patterns of $LiFePO_4$ and $FePO_4$ correspondingly

technique error, which is in reasonable agreement with the EDX result. The delithiated materials are isostructural orthorhombic $FePO_4$ from XRD patterns despite of the oxidant species. Rietveld refinement (Fig.1e) shows that the as-prepared $LiFePO_4$ has a larger crystallographic cell comparing with reported nano materials [10] because of the long time (24 h) sintering at the high temperature of 800 ℃. Such a synthesis condition therefore produces very large particle $LiFePO_4$ as shown in Fig.2a where the D_{50} in Fig.3a is about 12.61 μm. After chemical delithiation by NO_2BF_4, the particle size is slightly decreased as shown in Fig.2b and is further confirmed by laser particle size analyzer in Fig.3b where the D_{50} is about 10.28 μm with a narrower particle size distribution. Note that the particle size is dramatically decreased

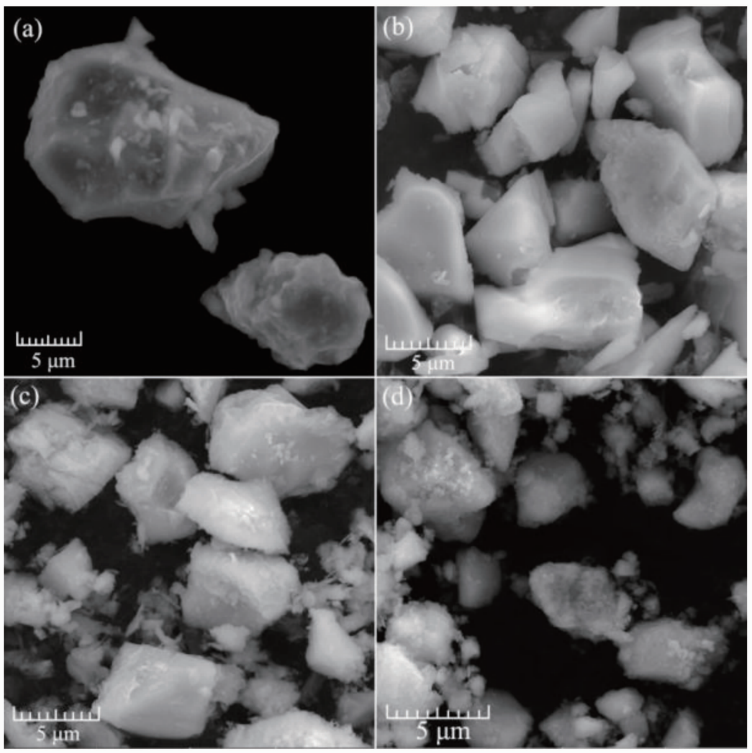

Fig.2　SEM images of pristine $LiFePO_4$ (a), $FePO_4$-N (b), $FePO_4$-K (c) and $FePO_4$-K-AN (d)

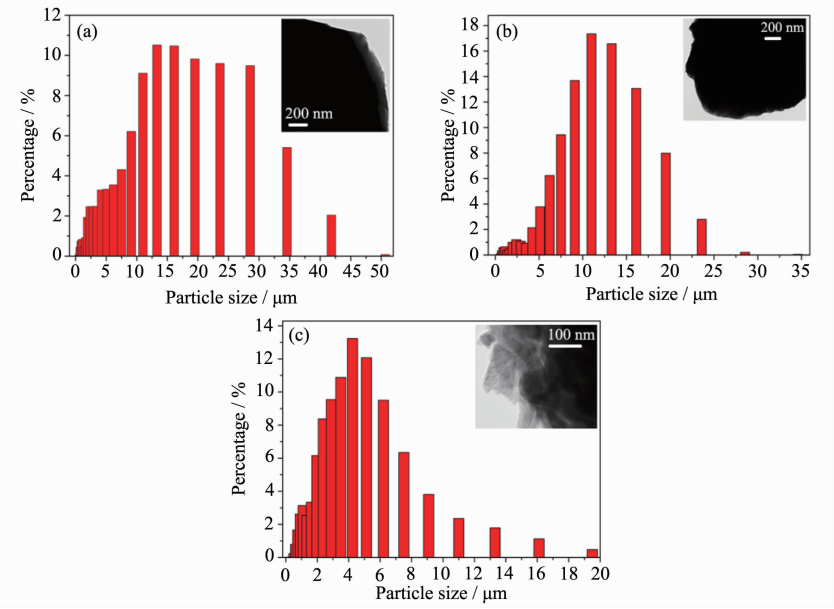

Insets exhibit their TEM images

Fig.3　Particle size distributions of pristine $LiFePO_4$ (a), $FePO_4$-N (b) and $FePO_4$-K (c)

for $FePO_4$ derived by $K_2S_2O_8$. The D_{50} is only 3.54 μm with a much narrower size distribution as shown in Fig.3c. This is consistent with Rietveld refinement that $FePO_4$-K has a smaller crystallographic cell than $FePO_4$-N (Fig.1e). More interestingly, there are many small and thin plates/whiskers on the particle surface of $FePO_4$-K in Fig.2c. TEM images (insets of Fig.3) clearly reflect the morphology difference of these samples. $FePO_4$-N nearly retains the round particle shape of pristine $LiFePO_4$, but the particle surface of

$FePO_4$-K seems seriously corroded or dissolved leaving many thin plates/whiskers on its surface. Structural fractures even crystallographic disorders and texture defaults [37] are then thought very probably formed in $FePO_4$-K.

CR2016 coin cells with Li metal as the anodes were fabricated to investigate the battery performance of these materials. Fig.4a shows the charge/discharge curves of pristine $LiFePO_4$, $FePO_4$-N and $FePO_4$-K at the current of 1C (means charged or discharged in 1 h) with a CC/CD mode (constant charge/constant discharge at the same rate) between 2.0 V and 4.3 V (vs. Li/Li^+ hereafter) at room temperature. The specific discharge capacity and coulombic efficiency (discharge capacity divided by charge capacity) of pristine $LiFePO_4$ are 63.12 mAh·g^{-1} and 91.72% respectively, which are reasonable considering the ultra large particle (12.61 μm vs. nano) without any modification such as surface coating or bulk doping. Moreover, it shows a flat charge/discharge plateau at 3.5/3.4 V in good agreement with literature [38-39]. The specific discharge capacity of $FePO_4$-N is a little promoted to 64.80 mAh·g^{-1} with the coulombic efficiency of 96.29% probably due to its smaller particle size. However, $FePO_4$-K shows totally different behavior. For one thing, both the charge and discharge curves are changed to slope-like profiles; for another, the specific discharge capacity decreases drastically to only 31.50 mAh·g^{-1}. The prototype batteries were further tested by a CCCV/CD mode between 2.5 V and 4.0 V at room temperature. They were charged constantly at C/5 rate to 4.0 V followed by a constant voltage charging to the current of C/25, and were discharged at C/5 again to 2.5 V. The results are shown in Fig.4b. At a lower rate plus constant voltage charging, the specific discharge capacity of pristine $LiFePO_4$, $FePO_4$-N and $FePO_4$-K are increased to 75.71 mAh·g^{-1}, 77.98 mAh·g^{-1} and 39.75 mAh·g^{-1} respectively exhibiting a similar change trend in capacity and voltage profiles as shown in Fig.4a by CC/CV tests. Fig.5 shows the room temperature EIS of different samples at fully charged state. The impedance spectrum is generally composed of a semicircle at high frequency and a sloping line at low frequency region roughly corresponding to the charge transfer impedance (R_{ct}) and the Warburg impedance related to lithium diffusion in the active material, respectively [40]. It therefore can be seen that the charge transfer impedance of $FePO_4$-K(R_{ct}=600 Ω) is much larger than that of pristine $LiFePO_4$ (R_{ct}=61 Ω) or that of $FePO_4$-N (R_{ct}=64 Ω), which agrees reasonably with the battery performance in Fig.4.

Remember that pristine $LiFePO_4$ is chemically delithiated by NO_2BF_4 in an organic solution (acetonitrile) but by $K_2S_2O_8$ in an aqueous solution (deionized water), the abnormal structure, morphology and electrochemical performance of $FePO_4$-K is probably correlated with solvent H_2O since partially hydrated olivine phase could lead to performance loss of $LiFePO_4$[41]. Even moisture or trace oxygen[42–44] could induce structure change and performance degradation of $LiFePO_4$, not to mention the long time (30 h) immersion of Li_xFePO_4 ($0 \leqslant x \leqslant 1$) here in H_2O under a highly oxidative environment. Fig.6 shows the FTIR

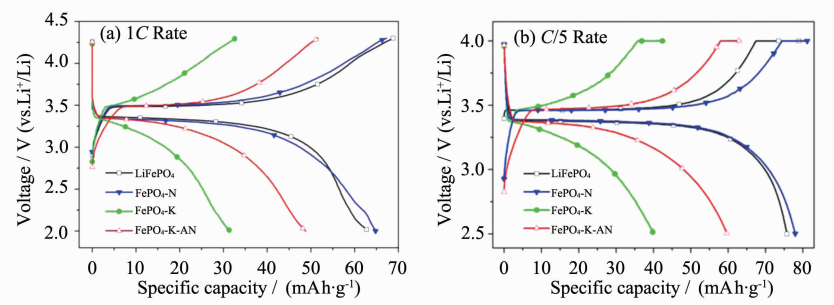

Fig.4 Charge/discharge curves of pristine $LiFePO_4$, $FePO_4$-N, $FePO_4$-K, and $FePO_4$-K-AN. The prototype batteries are tested by the CC/CD mode at 1C rate in (a) while by the CCCV/CD mode at C/5 rate in (b)

spectrum of $FePO_4$-K in comparison with that of $FePO_4$-N. In agreement with Juliens work [45-47], the peaks ranged from 940 cm^{-1} to 1 095 cm^{-1} correspond to the stretching modes of PO_4^{3-} units while that at 1 237 cm^{-1} corresponds to the vibration mode of PO_3. The peaks at 1 471 cm^{-1}, 2 855 cm^{-1} and 2 921 cm^{-1} are the deformation mode, symmetric stretching mode and asymmetric stretching mode of -CH_2 respectively [48]. They are mainly found in $FePO_4$-N because of the residual -C-H groups from acetonitrile. There is also a little -CH_2 in $FePO_4$-K because it was filtered alternately by water and ethanol. As can be seen in Fig.4, -CH_2 has little influence on the battery performance of Li_xFePO_4 ($0 \leqslant x \leqslant 1$) since the electrodes are soaked in organic electrolytes. The peak at 1 642 cm^{-1} shows the deformation mode of liquid H_2O with only a little amount that was not fully removed during drying. Note that the broad peak band at 3 500 cm^{-1}~2 500 cm^{-1} implies significant O-H groups in $FePO_4$-K, which is similar with layered oxide cathodes during chemical delithiation [49]. Manthirams group[50] found that layered compounds are favorable of protonation while olivine $LiFePO_4$ doesn't encounter such a problem in organic solutions as in the case of $FePO_4$-N. However, the large content of O-H groups in $FePO_4$-K indicates that it is possible for protons to incorporate into the crystal lattice of Li_xFePO_4 ($0 \leqslant x \leqslant 1$) in aqueous solutions.

Considering protonation during chemical delithiation, there are mainly three types of hydroxyls in $FePO_4$-K: the residual H_2O that was not fully removed by drying, lattice O-H groups in $FePO_4$ due to the inserted protons, and the adsorbed -OH concomitant with proton incorporation. There should be only a little residual H_2O as FTIR indicates at 1 642 cm^{-1} because the sample was dried under vacuum at 80 ℃ for 12 h, therefore, the significant O-H groups are mainly related with protonation during delithiation. Scheme 1 gives an illustration of the structure and morphology change along with chemical delithiation in aqueous solutions. When $LiFePO_4$ and $K_2S_2O_8$ are mixed together, the loose coupled particles are dispersed by vigorous stirring in addition with partial dissolution [51]. This causes the initial particle downsizing and roughening of $LiFePO_4$. While lithium is being removed, some protons are incorporated into the crystal lattice of Li_xFePO_4 ($0 \leqslant x \leqslant 1$) either by proton-lithium exchange or by proton insertion into lithium vacancies leading to surface corrosion (dissolution) and further decrease of the particle size. At the same time, the isolated -OH could be possibly adsorbed on the coarse surface of Li_xFePO_4 ($0 \leqslant x \leqslant 1$). Note that these processes take place simultaneously and multidimensionally, and their synergism

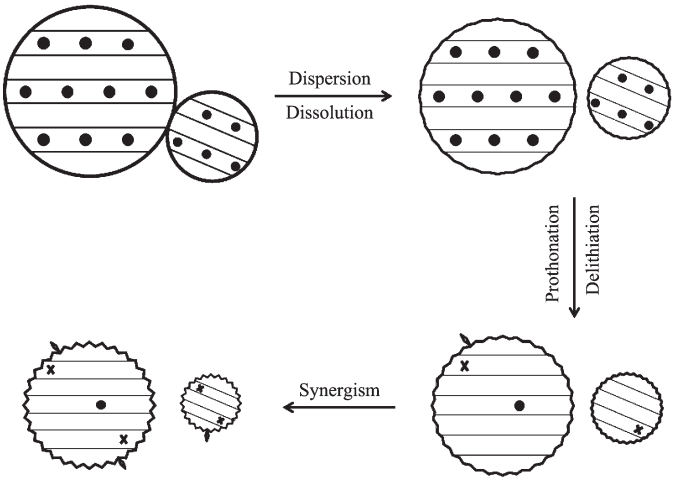

●, ×, and ◇ represents Li^+, H^+, and OH^- respectively while the circles indicate $LiFePO_4$ particles with different sizes and morphologies along with delithiation. The lithium channels are parallel to (010) indicating their diffusion path

Scheme 1　Schematic illustration of chemical delithiation of $LiFePO_4$ in aqueous solutions

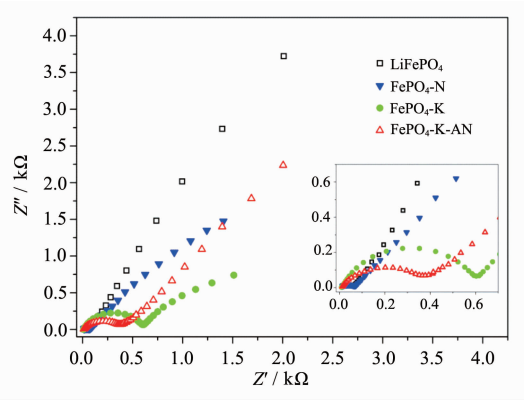

Fig.5 Room temperature EIS of $LiFePO_4$, $FePO_4$-N, $FePO_4$-K and $FePO_4$-K-AN at the fully charged state. The inset magnifies the high frequency region for clear illustration

accelerates the overall structure and morphology change of $FePO_4$-K as shown in Fig.2 and Fig.3. As a result, its battery performance is dramatically deteriorated, and the charge/discharge curves are changed to slope-like profiles. On the contrary, there are not much protons in acetonitrile, thus protonation is rarely involved in chemical delithiation of $LiFePO_4$ by NO_2BF_4. This comes to be the main difference of chemical delithiation of $LiFePO_4$ by the two oxidants. The slight particle size decrease of $FePO_4$-N is mainly caused by the long time dispersion of Li_xFePO_4 ($0 \leqslant x \leqslant 1$) under vigorous stirring and its light dissolution during chemical delithiation.

Post annealing was conducted to eliminate the residual water, hydroxyls and inserted protons in $FePO_4$-K. It is reported [6,52] that orthorhombic $FePO_4$ could be rearranged into trigonal $FePO_4$ at temperatures higher than 450 ℃. Therefore, $FePO_4$-K was annealed at 300 ℃ for 24 h under Ar protection in this paper. The content of O-H groups in $FePO_4$-K-AN is indeed decreased as shown in Fig.6. The XRD pattern in Fig.1d and the SEM image in Fig.2d demonstrate that the phase structure and particle morphology of $FePO_4$-K-AN have no much change comparing to $FePO_4$-K. Due to the removal of protons that could possibly block the 1D lithium diffusion channels, the specific discharge capacity is now improved to 48.81 mAh·g^{-1} in Fig.4a and 59.35 mAh·g^{-1} in Fig.4b, which are both higher than that of $FePO_4$-K but are still not as good as pristine $LiFePO_4$ (and $FePO_4$-N). The irrecoverable performance might be related with the irreversible changes such as structure fractures, crystallographic disorders and texture defaults during chemical delithiation. The R_{ct} value of $FePO_4$-K-AN is 360 Ω sitting between pristine $LiFePO_4$ ($FePO_4$-N) and $FePO_4$-K as shown in Fig.5. TGA-DSC (Fig.7) shows an intensive weight loss at 100~200 ℃ with an endothermic peak indicating the removal of H_2O and protons from $FePO_4$-K. There is still a gradual weight loss slowly extending to higher temperatures demonstrating further extraction of protons. The heat treatment is stopped at 400 ℃ to avoid phase transformation at higher temperatures[52]. It can be seen from TGA that the total weight loss is about 2% which is lower than the reported value (5.5%)[47] of $Li_{1-x}Ni_{0.5}Mn_{0.5}O_2$ because of the large distortion of the Fe and P coordination polyhedra in $LiFePO_4$[36].

In short, very large particle $LiFePO_4$ is synthesized in this paper to investigate the structure, morphology and performance difference of $FePO_4$ derived by chemical delithiation of $LiFePO_4$ with different oxidation systems. Large particles could give the intrinsic difference without the interference of size effects[10]. It is found that solvents are highly involved in chemical delithiation of $LiFePO_4$. Moreover, proton insertion into the crystal lattice of Li_xFePO_4 ($0 \leqslant x \leqslant 1$) is identified in $FePO_4$ derived by $K_2S_2O_8$. The synergism of dispersion, dissolution, delithiation and more importantly protonation during chemical delithiation makes the structure and morphology of

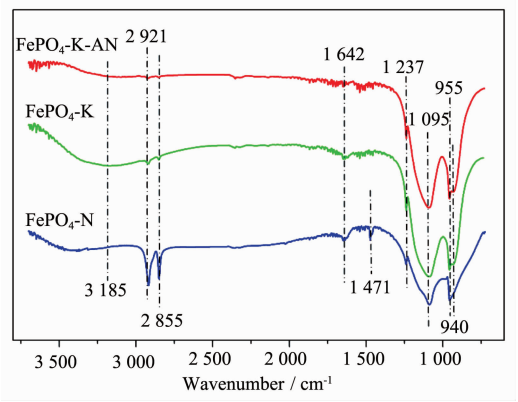

Fig.6 FTIR spectra of $FePO_4$-N, $FePO_4$-K and $FePO_4$-K-AN

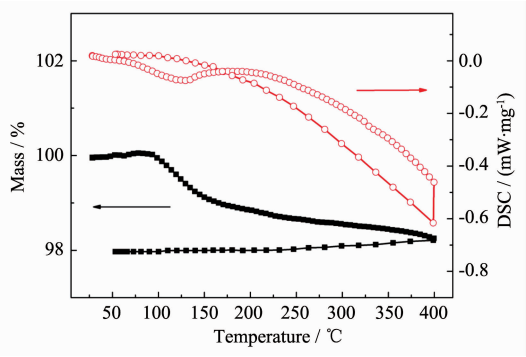

Fig.7　TGA-DSC curves of $FePO_4$-K from room temperature to 400 ℃ and backwards under a N_2 flow

$FePO_4$ dramatically deviate from pristine $LiFePO_4$. Consequently, the battery performance is seriously deteriorated. This work promotes careful control of chemical intrusion [27,34-35,53] into battery materials especially those are very subtle to atmosphere (such as $LiFePO_4$). At the same time, it indicates that proton insertion into the crystal lattice of Li_xFePO_4 ($0 \leqslant x \leqslant 1$) is possible in aqueous solutions when any critical condition such as oxidizability, pH, concentration, and immersion time is reached.

3　Conclusions

Solvents are found highly involved in chemical delithiation of $LiFePO_4$ and proton incorporation into Li_xFePO_4 ($0 \leqslant x \leqslant 1$) is demonstrated possible in highly oxidative aqueous solutions. The synergism of dispersion, dissolution, delithiation and protonation causes serious irreversible structure and morphology change to the derived $FePO_4$. As a result, the battery performance is dramatically degraded with increased charge transfer impedance and the charge/discharge curves are transformed to slope-like profiles. Further work needs to understand the detailed interaction between proton and Li_xFePO_4 ($0 \leqslant x \leqslant 1$) during charge/discharge.

Acknowledgements: Prof. Gerbrand Ceder at Massachusetts Institute of Technology is greatly appreciated for his kind instruction and fruitful discussion. The authors would also thank Dr. Ling Huang, Mrs. Lijing Ma and Mrs. Penghui Guo for technical help on TEM, XRD and FTIR, respectively.

References:

[1] Padhi A K, Nanjundaswamy K S, Goodenough J B. *J. Electrochem. Soc*., **1997**,**144**:1188-1194

[2] SUN Xiao-Fei(孙孝飞), XU You-Long(徐友龙), LIU Yang-Hao(刘养浩), et al. *Acta Phys.-Chim. Sin.* (物理化学学报), **2012**,**28**(12):2885-2892

[3] Sun X, Xu Y. *Mater. Lett*., **2012**,**84**:139-142

[4] Ellis B L, Lee K T, Nazar L F. *Chem. Mater.*, **2010**,**22**:691-714

[5] Whittingham M S. *Chem. Rev*., **2004**,**104**:4271-4302

[6] Yang S, Song Y, Zavalij P Y, et al. *Electrochem. Commun.*, **2002**,**4**:239-244

[7] Yang Z, Liu J, Baskaran S, et al. *JOM*, **2010**,**62**:14-23

[8] Goodenough J B, Kim Y. *Chem. Mater.*, **2010**,**22**:587-603

[9] CONG Chang-Jie(从长杰), ZHANG Xiang-Jun(张向军), LU Shi-Gang(卢世刚), et al. *Chinese J. Inorg. Chem.*(无机化学学报), **2011**,**27**(7):1319-1323

[10]Gibot P, Casas-Cabanas M, Laffont L, et al. *Nat. Mater*., **2008**,**7**:741-747

[11]Malik R, Burch D, Bazant M, et al. *Nano Lett*., **2010**,**10**:4123-4127

[12]Nakamura T, Miwa Y, Tabuchi M, et al. *J. Electrochem. Soc*., **2006**,**153**:A1108-A1114

[13]Zhu C, Yu Y, Gu L, et al. *Angew. Chem. Int. Ed*., **2011**,**50**:6278-6282

[14]GAO Fei(高飞), TANG Zhi-Yuan(唐致远), XUE Jian-Jun(薛建军). *Chinese J. Inorg. Chem.*(无机化学学报), **2007**,**23**(9):1603-1608

[15]Chung S Y, Bloking J T, Chiang Y M. *Nat. Mater*., **2002**,**1**:123-128

[16]Ying J R, Lei M, Jiang C Y, et al. *J. Power Sources*, **2006**,**158**:543-549

[17]DU Ke(杜柯), LIU Yan(刘艳), HU Guo-Rong(胡国荣), et al. *Chinese J. Inorg. Chem.*(无机化学学报), **2010**,**26**(7):1235-1239

[18]Kang B, Ceder G. *Nature*, **2009**,**458**:190-193

[19]Morgan D, Van der Ven A, Ceder G. *Electrochem. Solid-State Lett*., **2004**,**7**:A30-A32

[20]Islam M S, Driscoll D J, Fisher C A J, et al. *Chem. Mater*., **2005**,**17**:5085-5092

[21]DONG Jing(董静), ZHONG Ben-He(钟本和), ZHONG Yan-Jun(钟艳君), et al. *Chinese J. Inorg. Chem.*(无机化学学报), **2013**,**29**(18):0

[22]Nishimura S I, Kobayashi G, Ohoyama K, et al. *Nat. Mater*., **2008**,**7**:707-711

[23]Andersson A S, Thomas J O. *J. Power Sources*, **2001**,**97-98**:498-502

[24]Chen G, Song X, Thomas J R. *Electrochem. Solid-State Lett.*, **2006**,**9**:A295-A298

[25]Laffont L, Delacourt C, Gibot P, et al. *Chem. Mater.*, **2006**,**18**:5520-5529

[26]Delmas C, Maccario M, Croguennec L, et al. *Nat. Mater.*, **2008**,**7**:665-671

[27]Yamada A, Koizumi H, Sonoyama N, et al. *Electrochem. Solid-State Lett.*, **2005**,**8**:A409-A413

[28]Yamada A, Koizumi H, Nishimura S I, et al. *Nat. Mater.*, **2006**,**5**:357-360

[29]Gu L, Zhu C, Li H, et al. *J. Am. Chem. Soc.*, **2011**,**133**:4661-4663

[30]Malik R, Zhou F, Ceder G. *Nat. Mater.*, **2011**,**10**:587-590

[31]Bai P, Cogswell D A, Bazant M Z. *Nano Lett.*, **2011**,**11**:4890-4896

[32]Lin Q, Li Q, Gray K E, et al. *Cryst. Growth Des.*, **2012**,**12**:1232-1238

[33]Wu Y, Manthiram A. *J. Power Sources*, **2008**,**183**:749-754

[34]Delacourt C, Poizot P, Tarascon J M, et al. *Nat. Mater.*, **2005**,**4**:254-260

[35]Dodd J L, Yazami R, Fultz B. *Electrochem. Solid-State Lett.*, **2006**,**9**:A151-A155

[36]Benedek R, Thackeray M M, van de Walle A. *Chem. Mater.*, **2008**,**20**:5485-5490

[37]Sauvage F, Laffont L, Tarascon J M, et al. *Inorg. Chem.*, **2007**,**46**:3289-3294

[38]Matsui H, Nakamura T, Kobayashi Y, et al. *J. Power Sources*, **2010**,**195**:6879-6883

[39]Zhou F, Maxisch T, Ceder G. *Phys. Rev. Lett.*, **2006**,**97**:155704(4pages)

[40]Sun X, Xu Y, Jia M, et al. *J. Mater. Chem. A*, **2013**,**1**:2501-2507

[41]Cuisinier M, Martin J F, Dupré N, et al. *Electrochem. Commun.*, **2010**,**12**:238-241

[42]Martin J F, Cuisinier M, Dupré N, et al. *J. Power Sources*, **2011**,**196**:2155-2163

[43]Hamelet S, Casas-Cabanas M, Dupont L, et al. *Chem. Mater.*, **2011**,**23**:32-38

[44]Hamelet S, Gibot P, Casas-Cabanas M, et al. *J. Mater. Chem.*, **2009**,**19**:3979-3991

[45]Ait-Salah A, Jozwiak P, Zaghib K, et al. *Spectrochim. Acta Part A*, **2006**,**65**:1007-1013

[46]Ait-Salah A, Dodd J, Mauger A, et al. *Z. Anorg. Allg. Chem.*, **2006**,**632**:1598-1605

[47]Christopher M B, Roger F. *J. Electrochem. Soc.*, **2004**,**151**:A1032-A1038

[48]Stuart B H. *Infrared Spectroscopy: Fundamentals and Applications*. New York: Wiley, **2004**.

[49]Venkatraman S, Manthiram A. *J. Solid State Chem.*, **2004**,**177**:4244-4250

[50]Choi J, Alvarez E, Arunkumar T A, et al. *Electrochem. Solid-State Lett.*, **2006**,**9**:A241-A244

[51]Porcher W, Moreau P, Lestriez B, et al. *Electrochem. Solid-State Lett.*, **2008**,**11**:A4-A8

[52]Song Y N, Zavalij P Y, Suzuki M, et al. *Inorg. Chem.*, **2002**,**41**:5778-5786

[53]Delacourt C, Rodríguez-Carvajal J, Schmitt B, et al. *Solid State Sci.*, **2005**,**7**:1506-1516